A Crossover-UNIQUAC Model for Critical and Noncritical LLE Calculations

Khalil Parvaneh, Reza Haghbakhsh, and Alireza Shariati
Natural Gas Engineering Dept., School of Chemical and Petroleum Engineering, Shiraz University, Shiraz 71345, Iran

Cor J. Peters
Chemical Engineering Dept., The Petroleum Institute, Abu Dhabi, United Arab Emirates

Separation Technology Group, Dept. of Chemical Engineering and Chemistry, Eindhoven University of Technology, Den Dolech 2, 5612 AZ Eindhoven, The Netherlands

DOI 10.1002/aic.14948
Published online August 7, 2015 in Wiley Online Library (wileyonlinelibrary.com)

A new model, named the crossover-UNIQUAC model, has been proposed based on the crossover procedure for predicting constant-pressure liquid–liquid equilibria (LLE). In this manner, critical fluctuations were incorporated into the classical UNIQUAC equation. Coexistence curves were estimated for systems having a diverse range of asymmetries. These systems included the LLE of five different mixtures, composed of nitrobenzene with one of the members of the alkane homologous family (either pentane, octane, decane, dodecane, or tetradecane), as well as an extra system having a different chemical nature, namely the mixture of n-perfluorohexane and hexane, to further check the validity of the proposed approach. Using these nonideal mixtures, the validity of the new model was investigated within wide ranges, covering near-critical to regions falling far away from the critical point. The graphical trends, as well as the quantitative comparison with experimental data indicated the good agreement of the proposed model results with the experimental data. A maximum AARD% value of 3.97% was obtained in calculating molar compositions by the proposed model for such challenging systems covering noncritical, as well as critical regions. In addition, to show the strength of the proposed crossover approach to describe properties other than LLE, molar heat capacities were investigated for the system of nitrobenzene + dodecane. © 2015 American Institute of Chemical Engineers *AIChE J*, 61: 3094–3103, 2015
Keywords: UNIQUAC model, critical phenomena, liquid–liquid equilibria, crossover procedure, heat capacity

Introduction

A large number of the chemical industries are concerned with processes that include liquid–liquid equilibria (LLE).[1] For example, liquid–liquid extraction is among the main separation technologies used in the pharmaceutical and food industries.[2] Because of its significance to the industry, in order to describe LLE, various phenomenological and semitheoretical models have been proposed in the literature.[1] The regular solution model, Wilson model, NRTL model, and UNIQUAC model are among the commonly used models in literature, which are all based on classical mean-field theory. However, they fail to account for the effects of long-range concentration fluctuations in the vicinity of a consolute critical point. Indeed, the problem of classical models is that they predict the critical power-law behavior with incorrect classical critical exponents and fail to describe the singular behavior of thermodynamic properties in the critical region.[1,3] A near-critical system exhibits enhanced values of susceptibilities. As a liquid–liquid system approaches its critical point, the restoring force which drives a microscopic system into the equilibrium state disappeared.[3] Configurations different from the equilibrium configuration become long-lived, and the system displays patches where local values of concentration differ from the equilibrium values. The average value of this difference, that is, the concentration fluctuation, increases as the critical point is approached.[1,3]

Different system types, involving different molecular structures, show a common universal critical behavior near the critical point, because the correlation length near the critical point is very large compared with the molecular size. In this manner, the behavior of a system is determined by its collective critical behavior, not the type of molecule.[3,4]

Sufficiently close to the critical point, the properties vary according to a simple power of the temperature difference or concentration difference from the critical point, apart from the regular classical contribution. This means that, asymptotically close to the critical point, the thermodynamic properties satisfy scaling laws with universal critical exponents and universal scaling functions.[3,5]

The thermodynamic property, the path of approach to the critical point, and the universality class have the major roles

Additional Supporting Information may be found in the online version of this article.

Correspondence concerning this article should be addressed to C. J. Peters at cpeters@pi.ac.ae.

on the values of the universal exponents.[6] Fisher and coworkers[7,8] presented a formulation of complete scaling for one-component fluids. This formulation was a revision of the standard scaling theory. Later, Anisimov and coworkers[9–11] proposed complete scaling for incompressible and weakly compressible binary liquid mixtures. Binary LLE, shown as $T-x$ coexistence curves, may have asymmetrical behavior. Anisimov and coworkers[9–11] showed that a singular diameter of the liquid–liquid coexistence curves originates from two different sources: one is associated with a correlation between concentration and entropy while the other is a correlation between concentration and molar density, which generates a more significant singular term. Recently, Bertrand et al.[12] presented the connection between the theory of complete scaling and the field-theoretic treatment of asymmetric fluid criticality. Huang et al.[13] and Yin et al.[14–16] investigated the asymmetric criticality of coexistence curves for some substances. They concluded that the heat capacity has a significant role in determining the asymmetric criticality of coexistence curves by the complete scaling theory.[13–16]

The exponents of the power laws can also be calculated from classical models. The classical equations remain analytic at the critical point, however, they fail to describe the singular behavior of some thermodynamic properties.[4]

The range of validity of an asymptotic power law is extremely limited to a small region near the critical point. Further away from the critical point, corrections on the scaling terms must be considered.[4,17]

A theoretical procedure to consider the effects of the long-range fluctuations is provided by the renormalization group theory of critical phenomena. Different crossover models have been developed based on the renormalization group theory. The crossover models combine the correct asymptotic behavior near the critical point with the classical behavior far away from the critical point.[4,18] Different modifications of classical equations have been proposed, to describe both the critical region and regions far away from the critical point. De Pablo and Prausnitz[19] first presented a phenomenological correction to the classical equations and obtained a good representation of LLE in some binary and ternary systems.[1] To consider nonclassical behavior, De Pablo and Prausnitz[20,21] also applied a Fox transformation[22] and extended it to binary and ternary systems. The renormalization-group theory is a theoretical procedure to combine long-range fluctuations into a classical equation. The studies of Sengers et al.[23–25] have shown how long-range fluctuations can be incorporated into a Landau-type expansion.[1] Based on their work, the theory has been extended to the Carnahan–Starling–De Santis equation of state.[26] Edison et al. proposed a general transformation of temperature and the mole fraction variable in the Gibbs energy models for LLE.[1] Their proposed transformation has the ability to be applied to any classical Gibbs energy model.[1] Nicoll and coworkers[18,27,28] proposed a transformation of a classical Landau expansion to incorporate the effects of critical fluctuations for pure fluids and binary systems. Based on their work, Chen et al.[23,29] and Jin et al.[30] presented different approaches based on the renormalization group theory of critical phenomena. Van't Hof et al.[3] used the NRTL model and improved the general approach introduced by Edison et al.[1] and presented the crossover-NRTL model. They successfully applied their proposed model to a number of binary liquid systems at constant pressure.

Based on the model proposed by Van't Hof et al.[3] and a general approach presented by Edison et al.,[1] a new model, called the crossover-UNIQUAC model, is proposed in this work. The behavior and ability of the new model is investigated on six different liquid–liquid systems at constant pressure having coexistence curves of diverse asymmetries.

Theory

There are sufficient classical equations that can explain the behavior of fluids far away from their critical points. However, close to the critical point, other theories are necessary. Thermodynamic properties near the critical point can be related to the temperature differences or concentration differences with respect to the critical point. The crossover theory is used to smoothly join these two classes of equations.[31]

The thermodynamic properties near the critical point for a binary mixture can be described as follows[32]

$$\Delta\tilde{x}^{\mp} = \mp\ B_0\left|\frac{T-T_c}{T}\right|^{\beta} \tag{1}$$

$$\tilde{\chi}^{\mp} = \Gamma_0^{\mp}\left|\frac{T-T_c}{T}\right|^{-\gamma} \tag{2}$$

$$C_{Px}^{\mp} = A_0^{\mp}\left|\frac{T-T_c}{T}\right|^{-\alpha} \tag{3}$$

where B_0, $\Gamma_0^{\mp}$, and $A_0^{\mp}$ are system-dependent constants, T is the temperature, T_c is the critical temperature, and α, β, and γ are universal constants,[33] where $\Delta\tilde{x}=(x-x_c)/x_c$ and x_c is the molar fraction at the critical point. These critical constants are related by[33]

$$\gamma = 2-\alpha-2\beta \tag{4}$$

The power-law expansions are given in Table 1 for different paths.[33] The power law is valid in the vicinity of the critical point.[20]

As the equilibrium system moves to the region far away from critical region, classical thermodynamic theory is satisfactory and can explain the different behavior. The UNIQUAC model has been proposed for classical systems far away from the critical region.

UNIQUAC molar Gibbs energy of mixing

The molar Gibbs energy for a binary mixture of Components 1 and 2 at constant pressure has the following form

$$dG = -SdT+\mu_{21}dx \tag{5}$$

Where S is the molar entropy, $\mu_{21} = \mu_2-\mu_1$ and μ_i and x are the chemical potential of species i and the molar fraction ($x \equiv x_2$), respectively. The reduced molar Gibbs energy of mixing is

Table 1. Critical Power-Law Expansions[33]

Property	Power-Law Expansion	Path
$\tilde{c}_V = -\tilde{T}^2(\partial^2\tilde{A}/\partial\tilde{T}^2)_\rho$	$A^+\tau^{-\alpha}(1+A_1^+\tau^{\Delta_1}+...)$	$\Delta\rho=0,\tau\geq 0$
$\tilde{c}_V = -\tilde{T}^2(\partial^2\tilde{A}/\partial\tilde{T}^2)_\rho$	$A^-\lvert\tau\rvert^{-\alpha}(1+A_1^-\lvert\tau\rvert^{\Delta_1}+...)$	$\Delta\rho=0,\tau\leq 0$
$\tilde{\chi} = (\partial\tilde{\rho}/\partial\tilde{\mu})_T$	$\Gamma^+\tau^{-\gamma}(1+\Gamma_1^+\tau^{\Delta_1}+...)$	$\Delta\rho=0,\tau\geq 0$
$\tilde{\chi} = (\partial\tilde{\rho}/\partial\tilde{\mu})_T$	$\Gamma^-\lvert\tau\rvert^{-\gamma}(1+\Gamma_1^-\lvert\tau\rvert^{\Delta_1}+...)$	$\Delta\rho=\Delta\rho_{cxc}$, $\tau\leq 0$
$\Delta\tilde{\mu} = (\partial\Delta\tilde{A}/\partial\Delta\rho)_T$	$\pm D\lvert\Delta\rho\rvert^{\delta}(1+D_1\lvert\Delta\rho\rvert^{\Delta_1/\beta}+...)$	$\tau=0$
$\lvert\Delta\rho_{cxc}\rvert$	$B\lvert\tau\rvert^{\beta}(1+B_1\lvert\tau\rvert^{\Delta_1}+...)$	$\tau\leq 0$

$$\frac{\Delta g}{RT}=(1-x)\ \ln(1-x)+x\ \ln(x)+\frac{g^{E}}{RT} \tag{6}$$

where R and g^{E} are the universal gas constant and the excess Gibbs energy, respectively.

The universal quasi-chemical theory (or in short, UNIQUAC) is used in this work for describing the excess Gibbs energy. The UNIQUAC model is given by[34]

$$\frac{g^{E}}{RT}=\left(\frac{g^{E}}{RT}\right)^{\text{Comb.}}+\left(\frac{g^{E}}{RT}\right)^{\text{Res.}} \tag{7}$$

where $\left(\frac{g^{E}}{RT}\right)^{\text{Comb.}}$ and $\left(\frac{g^{E}}{RT}\right)^{\text{Res.}}$ are the combinatorial and residual terms, respectively

$$\begin{aligned}\left(\frac{g^{E}}{RT}\right)^{\text{Comb.}}&=(1-x)\ln\left(\frac{\Phi_1^{*}}{1-x}\right)+x\ \ln\left(\frac{\Phi_2^{*}}{x}\right)\\&+\frac{Z}{2}\left((1-x)q_1\ln\left(\frac{\theta_1}{\Phi_1^{*}}\right)+xq_2\ \ln\left(\frac{\theta_2}{\Phi_2^{*}}\right)\right)\end{aligned} \tag{8}$$

$$\left(\frac{g^{E}}{RT}\right)^{\text{Res.}}=-(1-x)q_1'\ln\left(\theta_1'+\theta_2'\tau_{21}\right)-xq_2'\ln\left(\theta_2'+\theta_1'\tau_{12}\right) \tag{9}$$

where

$$\Phi_1^{*}=\frac{(1-x)r_1}{(1-x)r_1+xr_2} \tag{10}$$

$$\Phi_2^{*}=\frac{xr_2}{(1-x)r_1+xr_2} \tag{11}$$

$$\theta_1=\frac{(1-x)q_1}{(1-x)q_1+xq_2} \tag{12}$$

$$\theta_2=\frac{xq_2}{(1-x)q_1+xq_2} \tag{13}$$

$$\theta_1'=\frac{(1-x)q_1'}{(1-x)q_1'+xq_2'} \tag{14}$$

$$\theta_2'=\frac{xq_2'}{(1-x)q_1'+xq_2'} \tag{15}$$

$$\tau_{12}=\exp\left(-\frac{\Delta u_{12}}{RT}\right)=\exp\left(-\frac{a_{12}}{T}\right) \tag{16}$$

$$\tau_{21}=\exp\left(-\frac{\Delta u_{21}}{RT}\right)=\exp\left(-\frac{a_{21}}{T}\right) \tag{17}$$

where r, q, and q' are the molecular-structure constants for each pure component. The parameter Z is the coordination number and is set to 10.[34]

All variables are made dimensionless by the following transformations[1]

$$\tilde{T}=-\frac{T_c}{T} \tag{18}$$

$$\tilde{x}=\frac{x}{x_c} \tag{19}$$

$$\tilde{g}=\frac{g}{RT} \tag{20}$$

$$\Delta\tilde{T}=1+\tilde{T} \tag{21}$$

$$\Delta\tilde{x}=\tilde{x}-1 \tag{22}$$

By applying the same method, τ_{12} and τ_{21} are

$$\tau_{12}=\exp\left(\tilde{c}\left(1+\tilde{d}\Delta\tilde{T}\right)\right) \tag{23}$$

$$\tau_{21}=\exp\left(\tilde{a}\left(1+\tilde{b}\Delta\tilde{T}\right)\right) \tag{24}$$

The number of parameters in Eqs. 23 and 24 are reduced by two parameters when applying the incipient immiscibility at the consolute critical point condition[1]

$$\left(\frac{\partial^2\Delta G}{\partial x^2}\right)\Big|_{x=x_c,\ T=T_c}=\left(\frac{\partial^3\Delta G}{\partial x^3}\right)\Big|_{x=x_c,\ T=T_c}=0 \tag{25}$$

From Eq. 25, the $\tilde{a}$ and $\tilde{c}$ parameters are given in terms of mole fraction at the critical point (x_c). These equations must be calculated for each system.

Crossover theory

A method was suggested by Edison et al.[1] to apply the crossover theory to classical Gibbs energy equations. The classical Gibbs energy of mixing is separated to singular and regular parts using a Taylor series around the mole fraction at the critical point[1]

$$\Delta\tilde{g}_{\text{cl}}(\tilde{T},\tilde{x})=\Delta\tilde{g}(\tilde{T},1)+\frac{\partial}{\partial\tilde{x}}\Delta\tilde{g}|_{\tilde{x}=1}(\tilde{x}-1)+\ldots \tag{26}$$

In this definition, the second and higher orders in $\tilde{x}$ are formed

$$\Delta\tilde{g}_{\text{cr}}(\tilde{T},\tilde{x})=\Delta\tilde{g}_{\text{cl}}(\tilde{T},\tilde{x})-\Delta\tilde{g}(\tilde{T},1)-\frac{\partial}{\partial\tilde{x}}\Delta\tilde{g}|_{\tilde{x}=1}(\tilde{x}-1) \tag{27}$$

Thus

$$\Delta\tilde{g}_{\text{reg}}(\tilde{T},\tilde{x})=\Delta\tilde{g}(\tilde{T},1)+\frac{\partial}{\partial\tilde{x}}\Delta\tilde{g}|_{\tilde{x}=1}(\tilde{x}-1) \tag{28}$$

When calculating $\Delta\tilde{g}_{\text{reg}}$ and $\Delta\tilde{g}_{\text{cr}}$, $x=x_c(1+\Delta\tilde{x})$, so $\Delta\tilde{g}_{\text{cr}}$ is a function of $\Delta\tilde{T}$ and $\Delta\tilde{x}$. For measuring the distance from the critical point, the parameter κ has been used. In classical theory κ_{cl}^2 is[1]

$$\kappa_{\text{cl}}^2=\frac{\partial^2\Delta\tilde{g}_{\text{cr}}}{\partial\Delta\tilde{x}^2} \tag{29}$$

To account the effect of fluctuation in the critical term of molar Gibbs energy, it has to be renormalized. One such method was proposed by Chen et al.[23,29] in which the order parameter for incompressible fluids is the concentration.

The renormalized dimensionless variables in the critical term and the Gibbs energy of mixing are

$$\Delta\tilde{T}_R=\Delta\tilde{T}\zeta u^{-0.5} \tag{30}$$

$$\Delta\tilde{x}_R=\Delta\tilde{x}D^{0.5}u^{0.25} \tag{31}$$

$$\Delta\tilde{g}_{\text{sing}}=\Delta\tilde{g}_{\text{cr}}(\Delta\tilde{x}\rightarrow\Delta\tilde{x}_R,\Delta\tilde{T}\rightarrow\Delta\tilde{T}_R)-\frac{1}{2}c_l^2\Delta\tilde{T}^2\kappa \tag{32}$$

The term $-\frac{1}{2}c_l^2\Delta\tilde{T}^2\kappa$ is the kernel term which accounts for the fluctuation-induced contribution to the Gibbs energy of mixing.[1]

Table 2. The Experimental Values of Critical Temperature, Critical Mole Fraction, Temperature Range, and Number of Data for the Different Systems of This Study

Systems	T_c	x_c	Temperature (K)	Ndp.	Reference
Nitrobenzene + Pentane	297.104	0.386	287.335–297.102	31	36
Nitrobenzene + Octane	293.052	0.505	283.069–293.049	30	37
Nitrobenzene + Decane	295.964	0.574	285.959–295.958	28	36
Nitrobenzene + Dodecane	300.368	0.630	290.236–300.365	27	38
Nitrobenzene + Tetradecane	304.940	0.676	294.858–304.939	34	39
n-Perfluorohexane + Hexane	295.690	0.361	289.419–295.674	10	40

Ndp. is the number of data points.

D, κ, ζ, and u rescaling functions and defined as follows

$$D = Y^{-\eta/\omega} \tag{33}$$

$$\kappa = \frac{v}{\alpha \bar{u} \Lambda}\left(Y^{\frac{2v-1}{v\omega}} - 1\right) \tag{34}$$

$$\zeta = Y^{\frac{2v-1}{v\omega}} \tag{35}$$

$$u = Y^{1/\omega} \tag{36}$$

where α, η, v, and ω are universal constants, which are given in Supporting Informaiton Table S1. Y is the crossover function which was calculated by the implicit function where[23,24]

$$1-(1-\bar{u})Y = \bar{u}\left[1+\left(\frac{\Lambda}{\kappa}\right)^2\right]^{0.5} Y^{1/\omega} \tag{37}$$

In which

$$\kappa^2 = \frac{Y^{\frac{1}{2\omega}}}{c_\rho^2}\kappa_{cl}^2\left(\Delta\tilde{x} \to \Delta\tilde{x}_R, \Delta\tilde{T} \to \Delta\tilde{T}_R\right) \tag{38}$$

c_ρ is a system-dependent parameter which is related to the Landau theory. Thus, the parameters c_t and c_ρ can be calculated from Landau theory in the following manner[35]

$$c_t = \frac{\tilde{G}_{12}(\tilde{a},\tilde{b},\tilde{c},\tilde{d})}{\sqrt{\tilde{G}_{04}(\tilde{a},\tilde{c})}}\sqrt{u^*\bar{u}\Lambda} \tag{39}$$

$$c_\rho = \sqrt{\frac{\tilde{G}_{04}(\tilde{a},\tilde{c})}{u^*\bar{u}\Lambda}} \tag{40}$$

where u^* is the fixed point coupling constant and $\tilde{G}_{i,j}$ is a derivative of the Gibbs energy of mixing i times $\Delta\tilde{T}$, and j times $\Delta\tilde{x}$, and evaluated at the critical point.[3]

Calculation of heat capacity

The crossover-UNIQUAC model can also predict caloric properties, such as the molar heat capacity at constant pressure and composition, $C_{P,x}$. The heat capacity can be represented by Eq. 41[3]

$$\begin{aligned}\frac{\Delta C_{P,x}}{R} &= \left(\frac{\partial \Delta H/R}{\partial T}\right)_{P,x} = -\frac{T}{R}\left(\frac{\partial^2 \Delta G}{\partial T^2}\right)_{P,x} \\ &= -T\left(\frac{\partial^2 T\Delta\tilde{G}_{\text{reg}}}{\partial T^2} + \frac{\partial^2 T\Delta\tilde{G}_{\text{sing}}}{\partial T^2}\right)_{P,x}\end{aligned} \tag{41}$$

where ΔH is the enthalpy of mixing. The other parameters have been defined earlier. To account for a background contribution to heat capacity, Edison et al.[1] suggested that an analytic background function of $\tilde{\mu}_0(\Delta\tilde{T})$ should be added to the regular part of the Gibbs energy of mixing, in the form of Eq. 42

$$\tilde{\mu}_0(\Delta\tilde{T}) = \sum_{j=0}^{4}\tilde{\mu}_{0j}(\Delta\tilde{T})^j \tag{42}$$

The arbitrary coefficients of $\tilde{\mu}_{00}$ and $\tilde{\mu}_{01}$ are related to the zero points of energy and entropy. The other coefficients of $\tilde{\mu}_{02}$, $\tilde{\mu}_{03}$, and $\tilde{\mu}_{04}$ are system-dependent and can be optimized based on experimental caloric properties data far away from the consolute point.[1,3]

Investigated Compounds

For investigating the proposed crossover-UNIQUAC model, five different binary liquid–liquid systems with increasing size of components, that is, with coexisting curves that display different degrees of asymmetry, have been selected and their equilibrium composition data at different temperatures collected from the literature.[36–40] These include liquid–liquid mixtures of nitrobenzene with either pentane, octane, decane, dodecane, or tetradecane, that is, different members of the homologous family of alkanes. Also a system having a different chemical nature, namely *n*-perfluorohexane + hexane, has been investigated to further check the validity of the proposed approach. The temperature range and the number of data available for each system are reported in Table 2. The experimental values of critical temperatures at various mole fractions of the investigated systems, necessary by the UNIQUAC crossover model, are also reported in Table 2.

As this new model predicts liquid–liquid behavior with the UNIQUAC model in regions far away from the critical point as a classical method, all of the corresponding UNIQUAC parameters are necessary. This includes the volume and surface area structural parameters as the principle parameters. These parameters have been reported for some systems in the literature, while for others, they were calculated in this work based on the UNIFAC group contribution method.[41,42] Table 3 summarizes the values of the UNIQUAC volume and surface

Table 3. UNIQUAC Volume and the Surface Area Structural Parameters for the Investigated Compounds

Compound	r	q	Reference
Nitrobenzene	4.1292	3.14	43
n-Perfluorohexane	7.704	6.924	42
Pentane	3.8254	3.316	41
Hexane	4.5	3.86	42
Octane	5.849	4.936	44
Decane	7.1974	6.016	41
Dodecane	8.5462	7.096	44
Tetradecane	9.895	8.176	41

Table 4. The Calculated Values of Parameters $\tilde{a}$ and $\tilde{c}$ in Eqs. 23 and 24 by the Incipient Immiscibility at the Consolute Critical Point Conditions for the Different Systems

System	$\tilde{a}$	$\tilde{c}$
Nitrobenzene + Pentane	0.0489	−0.751
Nitrobenzene + Octane	0.1407	−0.7849
Nitrobenzene + Decane	0.1586	−0.773
Nitrobenzene + Dodecane	0.1704	−0.7621
Nitrobenzene + Tetradecane	0.1781	−0.7518
n-Perfluorohexane + Hexane	−0.4376	−0.0085

Table 5. The Values of the Optimized Parameters for the Different Systems by the Crossover-UNIQUAC Model

System	Λ	$\bar{u}$	$\tilde{b}$	$\tilde{d}$
Nitrobenzene + Pentane	1.298	0.346	3.53	0.513
Nitrobenzene + Octane	1.166	0.3	3.569	0.5104
Nitrobenzene + Decane	1.397	0.333	3.539	0.519
Nitrobenzene + Dodecane	1.2	0.378	3.58	0.499
Nitrobenzene + Tetradecane	1.166	0.313	3.54	0.540
Common parameters for Nitrobenzene + Alkanes	1.1	0.32	3.54	0.51
n-Perfluorohexane + Hexane	1.5	0.413	−2.283	−6.003

area structural parameters for the compounds investigated in this study.

In addition, to study the capability of the proposed crossover approach to describe properties other than LLE, molar heat capacities of nitrobenzene + dodecane are investigated. For this purpose, the liquid–liquid heat capacity data by Utt et al.[45] for nitrobenzene + dodecane near the consolute point were used to compare wiht the results of the proposed model of this study.

Results and Discussion

Based on the explanations provided in the "Theory" section, the liquid–liquid behavior of six different systems has been investigated by the crossover-UNIQUAC model. After identifying the values of critical temperature and composition for each system (Table 2), the parameters $\tilde{a}$ and $\tilde{c}$ in Eqs. 23 and 24 need to be calculated. By applying the incipient immiscibility at the consolute critical point conditions in Eq. 25, these parameters were calculated as reported in Table 4 for each system.

In addition to the two parameters of $\tilde{a}$ and $\tilde{c}$, which are not optimized but calculated parameters, the model contains four optimized parameters. Two of which (Λ and $\bar{u}$) correspond to the critical region and the other two ($\tilde{b}$ and $\tilde{d}$) are designated for the region far away from the critical point. These parameters should be optimized simultaneously for each system. Optimization was carried out using the Genetic Algorithm (GA). The values of these optimized parameters are presented in Table 5 for all of the mixtures investigated.

As can be observed in this table for nitrobenzene + alkanes systems, the values of the optimized parameters, in the case of every parameter, do not vary significantly for the various alkane members, that is, with the carbon number of the alkane. It can be concluded that these values are globally optimized values. If they had been corresponding to local optima, their values could have been quite different from one another among the varying systems. Also, because the values of the optimized parameters were rather close to one another for the various nitrobenzene + alkanes systems, we also suggest one set of "common" parameters for the whole homologous family of nitrobenzene + *n*-alkanes, in order to make the treatment more flexible and transferable. This common parameter set is also presented in Table 5.

For the system of *n*-perfluorohexane + hexane, because of the differing nature of the system, especially the component *n*-perfluorohexane, the values of the optimized parameters are somewhat different than the previous systems investigated. However, all are within the same order of magnitude. The objective function used for the optimization process is shown by Eq. 43. This objective function is based on the experimental temperature and composition, to which the calculated values by the model are guided to approach by proper optimization

$$\chi^2\left(x_{i,p,\mathrm{cal}}, T_{i,\mathrm{cal}}\right) = \frac{1}{N-M}\left\{\sum_{j=1}^{L}\sum_{i=1}^{N}\frac{\left(x_{i,p,\mathrm{exp}}-x_{i,p,\mathrm{cal}}\right)^2}{\sigma_x^2} + \sum_{i=1}^{N}\frac{\left(T_{i,\mathrm{exp}}-T_{i,\mathrm{cal}}\right)^2}{\sigma_T^2}\right\} \tag{43}$$

N and M are the number of data points and the number of adjustable parameters, respectively. L is the number of phases and σ_j is the standard deviation property.

The graphical results of the model for the six investigated systems are presented in Figures 1–6. Each figure consists of

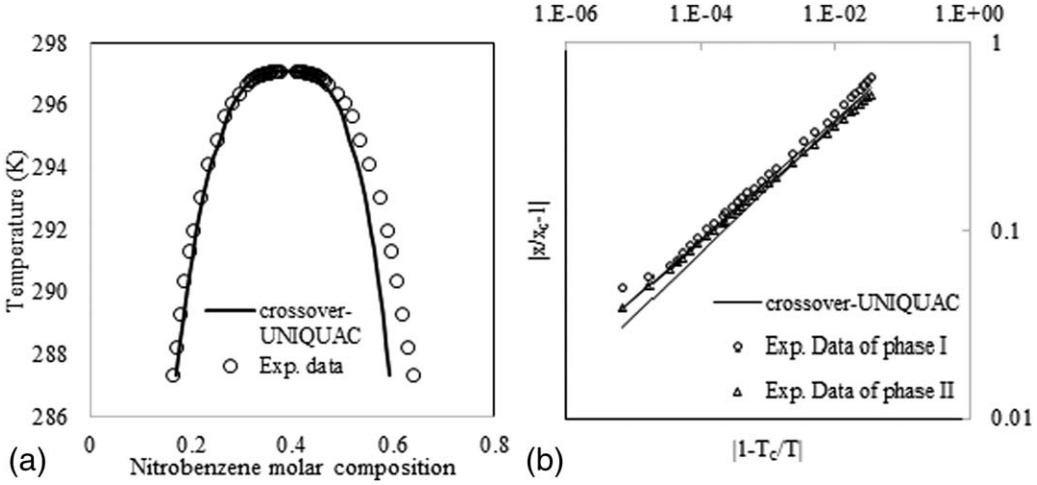

Figure 1. (a) Phase boundary of the binary nitrobenzene + pentane. (b) Log–log representation of experimental phase boundary data of both branches of the coexistence curve of nitrobenzene + pentane.

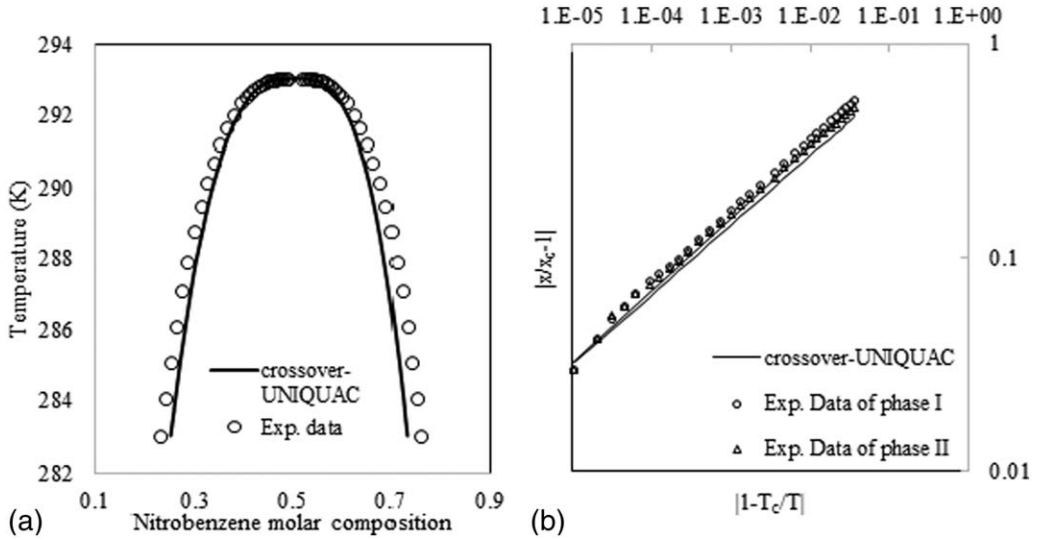

Figure 2. (a) Phase boundary of the binary system nitrobenzene + octane. (b) Log–log representation of experimental phase boundary data of both branches of the coexistence curve of nitrobenzene + octane.

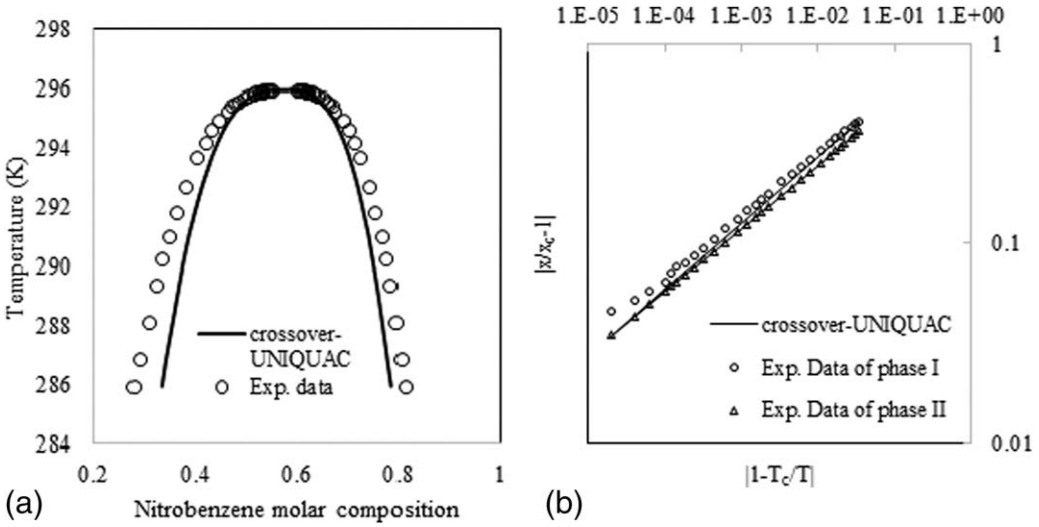

Figure 3. (a) Phase boundary of the binary liquid nitrobenzene + decane. (b) Log–log representation of experimental phase boundary data of both branches of the coexistence curve of nitrobenzene + decane.

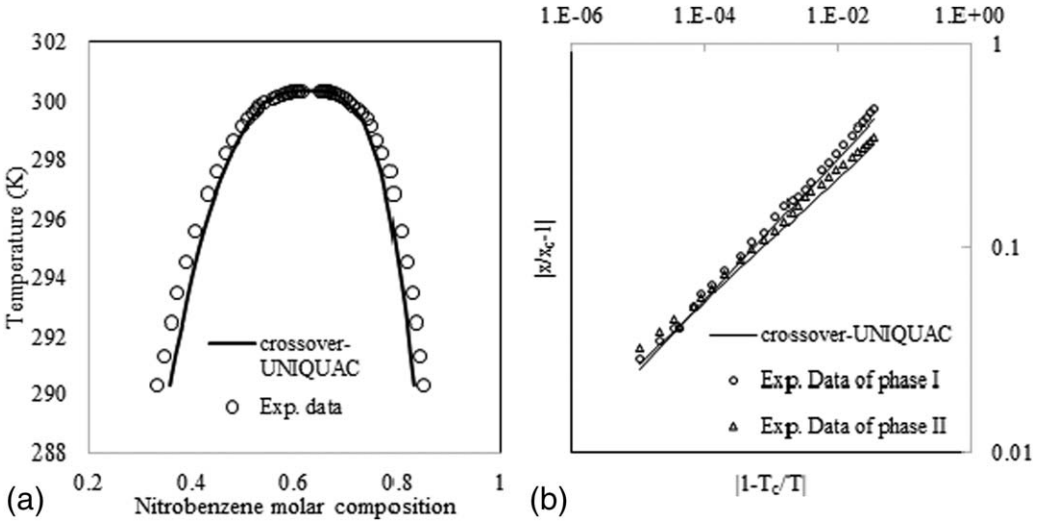

Figure 4. (a) Phase boundary of the binary system nitrobenzene + dodecane. (b) Log–log representation of experimental phase boundary data of both branches of the coexistence curve of nitrobenzene + dodecane.

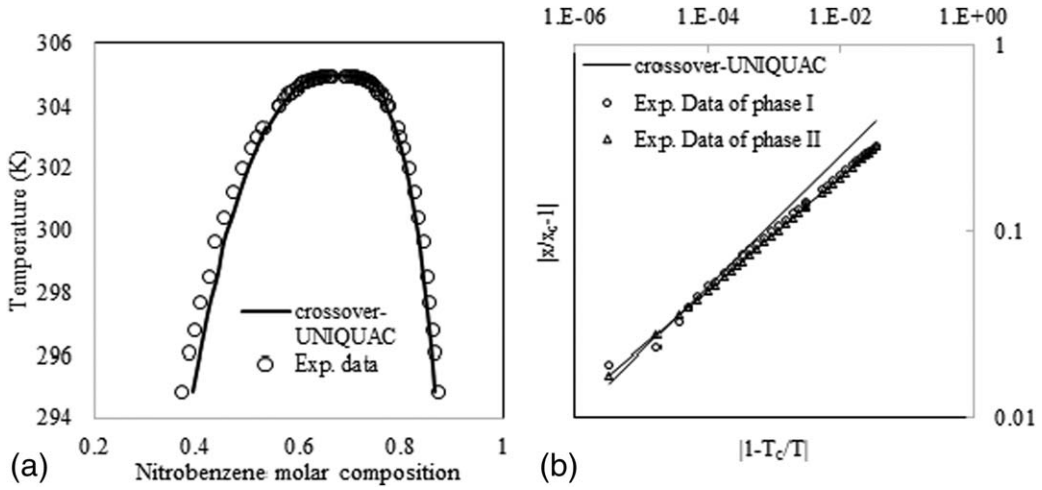

Figure 5. (a) Phase boundary of the binary system nitrobenzene + tetradecane. (b) Log–log representation of experimental phase boundary data of both branches of the coexistence curve of nitrobenzene + tetradecane.

two subfigures: the behavior of temperature vs. molar composition is shown in subfigure *a* for each of the systems.

As can be observed from these figures, the model results show good agreement with the experimental data. This agreement is particularly close in the critical region. It can be seen that, as the chain length of the alkane increases, the coexistence curve becomes more asymmetric. There are slight deviations far away from the critical region in the model with respect to experimental data. This is because only two optimized parameters have been used in the entire temperature range for each system, while in a conventional UNIQUAC model, a new set of optimized parameters are calculated at each different temperature.

According to Eq. 1, the limiting slopes of log–log plot of $\Delta \tilde{T}$ vs. $\Delta\tilde{x}$ on the two branches of the coexistence curve should be equal to the universal Ising value of the exponent β ($\beta = 0.3255$). Based on this fact, the log–log plots of different systems are presented as subfigures *b* in each of Figures 1–6. As can be seen, the limiting slopes of the two branches of the coexisting curve on the log–log plot are the same when approaching the critical point. However, further away from the critical point, the curves of the two branches of the coexistence curve start to diverge from one another because the distance to the critical point, $x - x_c$, is different for each branch.[3] Figure 6 shows a special behavior, differing from those given in Figures 1–5. This figure is the graphical validation of the proposed crossover-UNIQUAC model for a system of different nature. As can be seen from this figure, the results of the model are in good agreement with the experimental data and it can be concluded that the proposed model is also valid for systems having chemical natures that differ from those of the systems of Figures 1–5.

To have a comprehensive comparison between the conventional UNIQUAC model and the crossover-UNIQUAC model, the results of both of these models are compared in Figure 7 with experimental data for nitrobenzene + tetradecane as an example. As can be observed in Figure 7, the conventional UNIQUAC shows very large deviations from the experimental data for the near-critical to critical region. The other five systems investigated in this study have similar behavior. The graphical comparison of the conventional UNIQUAC and the crossover-UNIQUAC models are presented for these five systems in Supporting Information.

For a quantitative investigation of the proposed model, the values of the absolute average relative deviation (AARD%) of

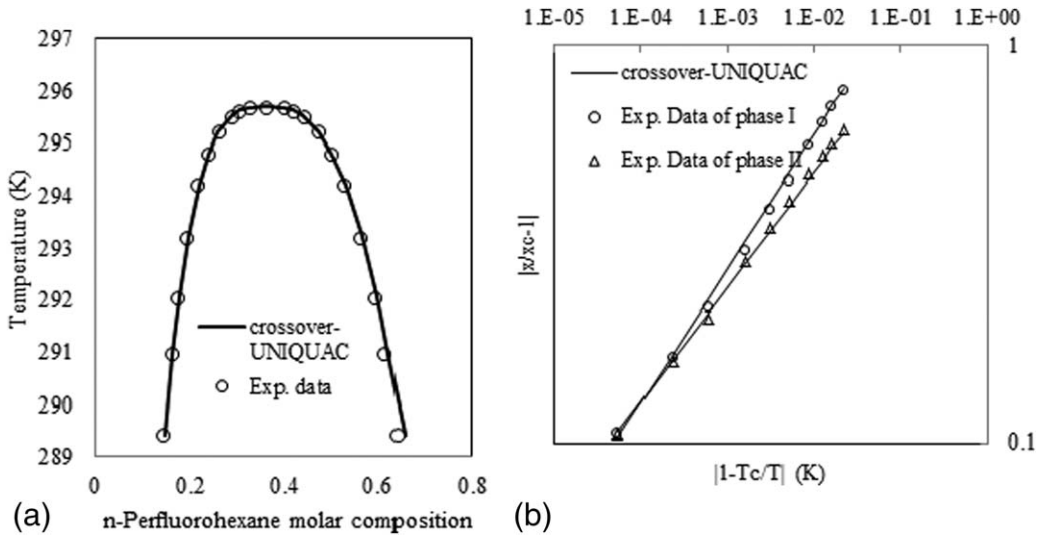

Figure 6. (a) Phase boundary of the binary system *n*-perfluorohexane + hexane. (b) Log–log representation of the experimental phase boundary data of both branches of the coexistence curve of *n*-perfluorohexane + hexane.

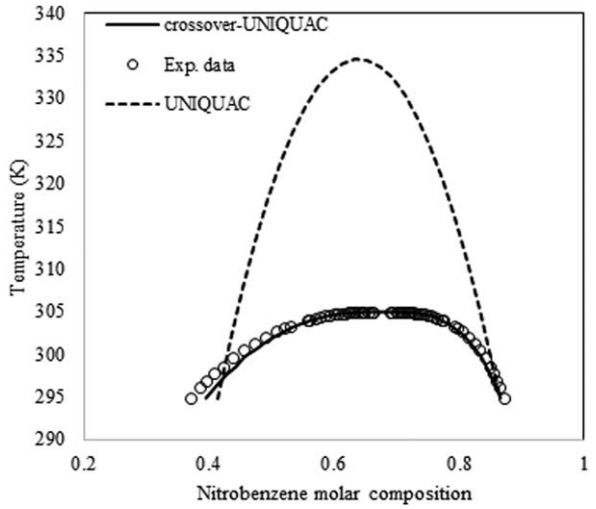

Figure 7. Liquid phase boundaries of the binary system of nitrobenzene + tetradecane by the conventional UNIQUAC and the crossover-UNIQUAC models.

the model results with respect to experimental data are reported in Table 6. This statistical error was calculated according to Eq. 44

$$\mathrm{AAD}=\frac{1}{N}\sum_{i=1}^{N}\left|100\left(\frac{x_{\mathrm{exp},i}-x_{\mathrm{cal},i}}{x_{\mathrm{exp},i}}\right)\right| \tag{44}$$

where N is the number of data points and $x_{\mathrm{exp},i}$ and $x_{\mathrm{cal},i}$ are the experimental and calculated mole fractions of component i, respectively.

Table 6 indicates that the maximum AARD% value is 3.97, belonging to the system of nitrobenzene + decane. Such quantitative comparisons of the proposed model show the good agreement of the model with experimental data, confirming the qualitative accuracy, previously shown by the graphical comparisons in Figures 1–6. The AARD% values, also for the crossover-UNIQUAC based on a common parameter set for all the nitrobenzene + alkanes systems, are presented in Table 6. These values do not differ much to the individual crossover-UNIQUAC errors because the values of the optimized parameters for each individual system are close to the common parameter set values.

The AARD% of the system of *n*-perfluorohexane + hexane is 1.21%. This is another evidence, from a quantitative point of view, in addition to qualitative results from Figure 6, confirming the validity of the proposed crossover-UNIQUAC model for a system of different nature.

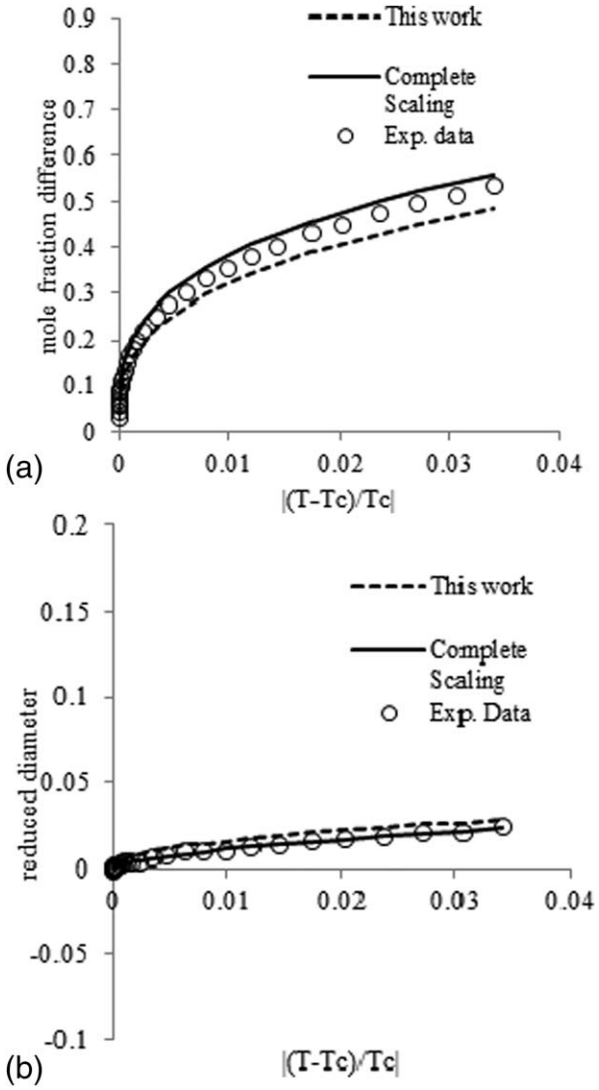

Figure 8. (a) Mole fraction difference $[(x' - x'')/2x_c]$ of the binary system of nitrobenzene + octane as a function of $|(T - T_c)/T_c|$. (b) The reduced diameter $[(x' + x'')/2x_c]$ for the coexistence curve of nitrobenzene + octane as a function of $|(T - T_c)/T_c|$.

The crossover-UNIQUAC model of this work is also compared with the crossover-NRTL model, as presented by Van't Hof et al.[3] In both crossover models, it is necessary to optimize two adjustable parameters for the whole temperature range. However, in the crossover-UNIQUAC model, the two adjustable parameters are included in only the residual part (Eq. 9), and not the combinatorial term of the excess Gibbs

Table 6. The Values of AARD% Calculated by the UNIQUAC-Crossover Model for the Different Systems and Comparison with the Corresponding Results of the Crossover-NRTL and Complete Scaling Model

System	AARD% Crossover-UNIQUAC	AARD% Crossover-NRTL[3]	AARD% Complete Scaling	AARD% Crossover-UNIQUAC with Common Parameters
Nitrobenzene + Pentane	2.19	0.44	0.66	2.73
Nitrobenzene + Octane	2.45	0.23	2.37	4.12
Nitrobenzene + Decane	3.97	0.49	2.09	4.01
Nitrobenzene + Dodecane	1.87	0.31	1.55	2.38
Nitrobenzene + Tetradecane	1.15	0.46	0.61	3.43
n-Perfluorohexane + Hexane	1.21	–	0.37	–

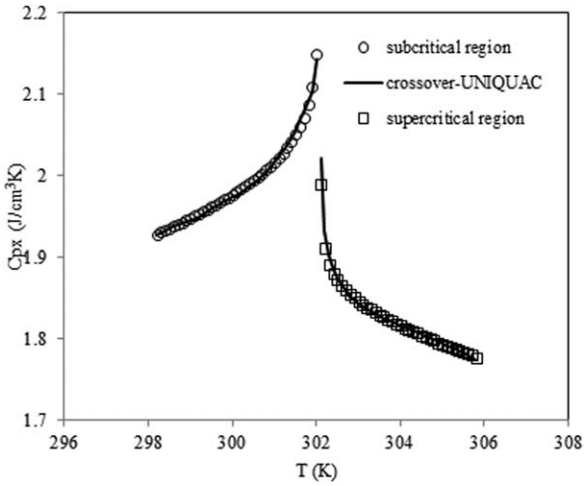

Figure 9. Comparison of the proposed crossover-UNIQUAC model results and the experimental molar heat capacities of nitrobenzene + dodecane at the composition x_c as a function of temperature in both subcritical and supercritical regions.

energy relation (Eq. 7). Therefore, less fitting is carried out in the case of the crossover-UNIQUAC, as compared with the crossover-NRTL. As a result, slightly larger deviations are expected for the crossover-UNIQUAC model, as confirmed in Table 6, which also includes the results of crossover-NRTL for comparison with the crossover-UNIQUAC.

The results of the scaling method of this work are also compared with those by the theory of complete scaling, as given by Cerdeirina et al.[9] Figure 8 presents the results for the system of nitrobenzene and octane.

As can be seen from Figure 8, both models agree well close to the critical points. The models start to deviate from one another as the distance to the critical point is increased. Such behavior is expected because both of the scaling models are derived for the very close vicinity of the critical point, and thus are more accurate in this region. Further systems are also compared in Supporting Informaiton Figures S6–S10. Although most figures show a better fit by the complete scaling model (Supporting Informaiton Figures S6 and S8), a definite generalization cannot be made as there are also examples in which the two models nearly coincide (Supporting Informaiton Figure S7) or where the scaling model of this work gives a better representation of the experimental data (Supporting Informaiton Figure S9).

As the Kernel term is included in the proposed crossover-UNIQUAC model, caloric properties, such as heat capacity, can also be investigated. For this purpose, experimental heat capacities of the system of nitrobenzene + dodecane have been selected from the literature for comparison with the model. The results of the proposed crossover-UNIQUAC model in Figure 9 show good agreement with the corresponding experimental values. The experimental heat capacities are presented in two regions, subcritical and supercritical, having a discontinuity at the consolute point. As can be seen from this figure, the proposed crossover-UNIQUAC has good agreement with the experimental data in both regions, while implying a weak divergence in $C_{P,x}$ at the consolute point. The system-dependent coefficients of $\tilde{\mu}_{02}$, $\tilde{\mu}_{03}$, and $\tilde{\mu}_{04}$, related to the heat capacity calculations are optimized in both regions and are presented in Table 7. The values of the corresponding coefficients in both regions are close to one another.

Table 7. The Values of the System-Dependent Coefficients, $\tilde{\mu}_{02}$, $\tilde{\mu}_{03}$, and $\tilde{\mu}_{04}$ in Eq. 42

Region	$\tilde{\mu}_{02}$	$\tilde{\mu}_{03}$	$\tilde{\mu}_{04}$
Two phase (subcritical)	−0.416	0.807	31.344
One phase (supercritical)	−0.339	0.593	35.974

Conclusions

In this study, a new model, based on existing crossover procedures has been proposed to incorporate critical fluctuations into the classical UNIQUAC equation to model constant-pressure liquid–liquid phase behavior, with coexistence curves of diverse asymmetries. Five different liquid–liquid systems at constant pressure, including mixtures of nitrobenzene with five different members of the alkane homologous family, that is, pentane, octane, decane, dodecane, and tetradecane were selected to investigate the validity of the new model. Also, a system of differing chemical nature, namely *n*-perfluorohexane + hexane, was investigated to show the validity of the proposed crossover-UNIQUAC for other systems. The GA procedure was used for optimization of the necessary parameters. The results of the proposed model showed good agreement with experimental data for every single system. The maximum AARD% obtained among the investigated systems was 3.97%, which indicates the high accuracy and reliability of the model. The graphical comparison of the model to experimental data, aimed at investigating the trend of the model in both the near-critical region and the region far away from criticality, was also presented. These results indicated that the model can have even better estimations in the critical region than it does further away from the critical point. Log–log plots of dimensionless molar composition and temperature with respect to critical molar composition and critical temperature, respectively, were prepared for the different systems investigated. It was concluded that the two branches of the coexistence curve behave similarly while closely approaching the critical point, but away from the critical point, these two branches start to diverge from one another.

Also, it was concluded that as the chain length of the alkane increases, the coexistence curve becomes more asymmetric, as observed in both the experimental data and by the results of the proposed model. The values of the optimized parameters for the different systems are reported. A comparison of these values for each parameter in the different systems show a rather consistent value, which does not vary much among the different systems composed of differing alkanes. Thus, it was concluded that these values correspond to globally optimized parameters. Furthermore, one set of "common" parameters is suggested for the whole homologous family of nitrobenzene + *n*-alkanes, in order to make the treatment more general.

For a more comprehensive investigation of the proposed crossover-UNIQUAC model, the caloric property of molar heat capacity was calculated close to the consolute point for the system of nitrobenzene + dodecane. The results showed good agreement between the heat capacities calculated by the model and the corresponding experimental data in both the subcritical and supercritical regions. The discontinuity near the consolute point was also observed.

Literature Cited

1. Edison TA, Anisimov MA, Sengers JV. Critical scaling laws and an excess Gibbs energy model. *Fluid Phase Equilib*. 1998;150–151: 429–438.
2. Casas LM, Orge B, Diaz C, Tojo J. Liquid–liquid equilibria for mixtures of {methyl acetate + methanol + *n*-alkane (C10–C12)} at several temperatures and 1 atm. *J Chem Thermodyn*. 2004;36:237–243.
3. Van't Hof A, Japas ML, Peters CJ. Description of liquid–liquid equilibria including the critical region with the crossover-NRTL model. *Fluid Phase Equilib*. 2001;192:27–48.
4. Hof Av. *Description of Liquid-Liquid Equilibria including the Critical Region with the Crossover-NRTL Model*. M.Sc. Thesis. Delft, The Netherlands: Laboratory for Applied Thermodynamics and Phase Equilibria, Faculty of Applied Sciences, Delft University of Technology, 2000.
5. Widom B. Equation of state in the neighborhood of the critical point. *J Chem Phys*. 1965;43:3898.
6. Anisimov MA, Povodyrev AA, Sengers JV. Crossover critical phenomena in complex fluids. *Fluid Phase Equilib*. 1999;158–160:537–547.
7. Fisher ME, Orkoulas G. The Yang-Yang anomaly in fluid criticality: experiment and scaling theory. *Phys Rev Lett*. 2000;85:696–699.
8. Orkoulas G, Fisher ME, Ustun C. The Yang–Yang relation and the specific heats of propane and carbon dioxide. *J Chem Phys*. 2000; 113:7530–7545.
9. Cerdeirina CA, Anisimov MA, Sengers JV. The nature of singular coexistence-curve diameters of liquid–liquid phase equilibria. *Chem Phys Lett*. 2006;424:414–419.
10. Wang JT, Cerdeirina CA, Anisimov MA, Sengers JV. Principle of isomorphism and complete scaling for binary-fluid criticality. *Phys Rev E*. 2008;77:031127.
11. Perez-Sanchez G, Losada-Perez P, Cerdeirina CA, Sengers JV, Anisimov MA. Asymmetric criticality in weakly compressible liquid mixtures. *J Chem Phys*. 2010;132:154502.
12. Bertrand CE, Nicoll JF, Anisimov MA. Comparison of complete scaling and a field-theoretic treatment of asymmetric fluid criticality. *Phys Rev E*. 2012;85:031131.
13. Huang M, Lei Y, Yin T, Chen Z, An X, Shen W. Heat capacities and asymmetric criticality of coexistence curves for benzonitrile + alkanes and dimethyl carbonate + alkanes. *J Phys Chem B*. 2011;115:13608–13616.
14. Yin TX, Lei YT, Huang MJ, Chen ZY, An XQ, Shen WG. Critical behavior of binary mixtures of nitrobenzene + *n*-undecane and nitrobenzene + *n*-dodecane. *J Solution Chem*. 2012;41:1866–1888.
15. Yin TX, Xu C, Lv H, Liu S, Wang M, Chen Z, Shen W. Asymmetric criticality of binary ionic solutions containing 1-butyl-3-methylimidazolium tetrafluoroborate and alcohol. *Phys Chem Chem Phys*. 2014;16:17715–17723.
16. Yin T, Liu S, Xie J, Shen W. Asymmetric criticality of the osmotic compressibility in binary mixtures. *J Chem Phys*. 2013;138:024504.
17. Sengers JMHL, Sengers JV, Raveché HJ. *Perspectives in Statistical Physics*. Amsterdam: North-Holland, 1981:238.
18. Nicoll JF, Albright PC. Crossover functions by renormalization-group matching: three-loop results. *Phys Rev B*. 1985;31:4576–4589.
19. De Pablo JJ, Prausnitz JM. Thermodynamics of liquid-liquid equilibria including the critical region. *AIChE J*. 1988;34:1595–1606.
20. De Pablo JJ, Prausnitz JM. Liquid-liquid equilibria for binary and ternary systems including the critical region. Transformation to non-classical coordinates. *Fluid Phase Equilib*. 1989;50:101–131.
21. De Pablo JJ, Prausnitz JM. Thermodynamics of liquid-liquid equilibria including the critical region. Transformation to non-classical coordinates using revised scaling. *Fluid Phase Equilib*. 1990;59:1–14.
22. Fox J. Method for construction of non-classical equations of state. *Fluid Phase Equilib*. 1983;14:45–53.
23. Chen ZY, Abbaci A, Tang S, Sengers JV. Global thermodynamic behavior of fluids in the critical region. *Phys Rev A*. 1990;42:4470–4484.
24. Anisimov MA, Kiselev SB, Sengers JV, Tang S. Crossover approach to global critical phenomena in fluids. *Physica A*. 1992;188:487–525.
25. Sengers JV, Kiran E, Levelt Sengers JMH. *Supercritical Fluids: Fundamentals for Application*. Dordrecht, The Netherlands: Kluwer, 1994:231–271.
26. Pelt Av, Jin GX, Sengers JV. Critical scaling laws and a classical equation of state. *Int J Thermophys*. 1994;15:687–697.
27. Nicoll JF. Critical phenomena of fluids: Asymmetric Landau-Ginzburg-Wilson model. *Phys Rev A*. 1981;24:2203.
28. Nicoll JF, Bhattacharjee JK. Crossover functions by renormalization-group matching: O(ε2) results. *Phys Rev B*. 1981;23:389.
29. Chen ZY, Albright PC, Sengers JV. Crossover from singular critical to regular classical thermodynamic behavior of fluids. *Phys Rev A*. 1990;41:3161.
30. Jin GX, Tang S, Sengers JV. Global thermodynamic behavior of fluid mixtures in the critical region. *Phys Rev E*. 1993;47:388.
31. Edison TA, Sengers JV. Thermodynamic properties of ammonia in the critical region. *Int J Refrig*. 1999;22:365–378.
32. Kumar A, Krishnamurthy HR, Gopal ESR. Equilibrium critical phenomena in binary liquid mixtures. *Phys Rep*. 1983;98:57.
33. Kiselev SB, Sengers JV. An improved parametric crossover model for the thermodynamic properties of fluids in the critical region. *Int J Thermophys*. 1993;14(1):1–32.
34. Prausnitz JM, Lichtenthaler RN, Azevedo EG. *Molecular Thermodynamics of Fluid-Phase Equilibria*, 3rd ed. Englewood Cliff: Prentice Hall PTR, 1999.
35. Edison TA. Thermophysical Properties of Fluids and Fluid Mixtures: Including Critical Fluctuations Effects, Ph.D. Thesis. University of Maryland, 1998.
36. An X, Li P, Zhao H, Shen W. The coexistence curves of $\{x C_6H_5NO_2 + (1-x)\ CH_3(CH_2)_3CH_3\}$ and and $\{x C_6H_5NO_2 + (1-x)\ CH_3(CH_2)_8CH_3\}$ in the critical region. *J Chem Thermodyn*. 1998;30: 1049–1059.
37. An X, Jiang F, Zhao H, Chen C, Shen W. Measurements of coexistence curves and turbidity for $\{x C_6H_5NO_2H + (1-x)\ CH_3(CH_2)_6CH_3\}$ in the critical region. *J Chem Thermodyn*. 1998;30: 751–760.
38. An X, Zhao H, Jiang F, Shen W. The coexistence curves of $\{x C_6H_5NO_2 + (1-x)\ CH_3(CH_2)_{10}CH_3\}$ in the critical region. *J Chem Thermodyn*. 1998;30:21–26.
39. An X, Zhao H, Jiang F, Mao C, Shen W. The coexistence curves of $\{x C_6H_5NO_2 + (1-x)\ CH_3(CH_2)_{12}CH_3\}$ in the critical region. *J Chem Thermodyn*. 1997;29:1047–1054.
40. Khairuin RA, Stankus SV, Gruzdev VA. Liquid-liquid coexistence curve of *n*-perfluorohexane-hexane system. *Int J Thermophys*. 2007; 28:1245–1254.
41. Smith JM, Van Ness HC, Abbott MM. *Introduction to Chemical Engineering Thermodynamics*, 6th ed. Boston: McGraw-Hill, 2001.
42. Gmehling J, Li J, Schiller M. A modified UNIFAC model. 2. Present parameter matrix and results for different thermodynamic properties. *Ind Eng Chem Res*. 1993;32:178–193.
43. Gao X, Yang Z, Xia S, Ma P. Liquid–liquid equilibrium data for binary systems containing *o*-dichlorobenzene and nitrobenzene. *Fluid Phase Equilib*. 2015;385:175–181.
44. Santiagoa RS, Santos GR, Aznar M. UNIQUAC correlation of liquid–liquid equilibrium in systems involving ionic liquids: the DFT–PCM approach. *Fluid Phase Equilib*. 2009;278:54–61.
45. Utt NJ, Lehman SY, Jacobs DT. Heat capacity of the liquid-liquid mixture nitrobenzene and dodecane near the critical point. *J Chem Phys*. 2007;127:104505.

Manuscript received Dec. 23, 2014, and revision received June 22, 2015.